

# Experimental Validation of a Heat Pump Model for B-Segment Electric Vehicles at Component Level

*Marie Peeters<sup>a</sup>, Elise Neven<sup>a</sup>, Vincent Lemort<sup>a</sup> and Samuel Gendebien<sup>a</sup>*

<sup>a</sup> *University of Liège, Liège, Belgium, marie.peeters@uliege.be*

<sup>a</sup> *University of Liège, Liège, Belgium, elise.neven@uliege.be*

<sup>a</sup> *University of Liège, Liège, Belgium, vincent.lemort@uliege.be*

<sup>a</sup> *University of Liège, Liège, Belgium, sgendebien @uliege.be*

## Abstract:

This paper presents the experimental validation of component-level models of an air-to-air heat pump used in a B-segment electric vehicle, based on measurements obtained from a dedicated test bench. The system consists of three heat exchangers (one outdoor and two in the so-called HVAC unit), a scroll compressor, valves, and an accumulator. This three-exchanger layout provides cabin cooling, cabin heating, and dehumidification capability while avoiding refrigerant-flow reversal. The working fluid is R1234yf. This dedicated test bench was conceived as a didactic platform for teaching technical thermodynamics and vehicle thermal-management principles. Developed within a project-based learning framework, the bench was designed, assembled, and commissioned by engineering students, and has since been used as a hands-on educational tool. In this work, component-level models of the heat pump were developed by students using Engineering Equation Solver (EES), based on physical modeling approaches. Experimental data collected on the test bench during laboratory sessions were used to calibrate and validate these models. Comparison between simulated and measured data demonstrates the ability of the component-level models to reproduce the system's performance across different operating conditions, providing a reliable tool for both research and educational purposes.

## Keywords:

Heat pump; Electric vehicle; HVAC; Thermal management; Experimental validation; Test bench; Component-level modeling; Project-based learning

## 1. Introduction

### 1.1 Context

Europe's energy transition is driving the large-scale deployment of electric vehicles (EVs) and promoting low-carbon energy solutions. Although the transport sector has achieved emission reductions over the past decades, it remains the largest source of greenhouse gas emissions in the European Union in 2025 according to the European Environment Agency [1]. The land transport sector has a strong potential for rapid transformation due to its relatively short operational lifetime compared to power plants [2]. Consequently, there is a growing interest in the thermal management of EV systems, including Air Conditioning (AC), batteries, powertrain components, and auxiliary equipment, as these directly impact driving range, component lifetime, and overall efficiency [3]. AC has become an essential feature for ensuring passenger comfort and safety. However, in electric vehicles, its use significantly affects battery autonomy, representing a key limitation of the technology, as highlighted in [4]. Unlike internal combustion engine vehicles, electric motors generate very little waste heat, meaning that free thermal energy is not readily available for cabin heating. In this context, reversible heat pumps are now widely adopted in electric vehicles to provide both heating and cooling, offering higher efficiency than conventional resistive heating systems.

### 1.2 Motivation and Objectives

From a research perspective, the objective of this work is to develop component-level models of key elements of an EV reversible AC system, such as the compressor and heat exchangers, and to experimentally validate them. The reliability of such models depends on their validation under realistic operating conditions. To this

end, experimental data collected on a dedicated test bench are used to assess the models through direct comparison between simulated and measured results.

From an educational standpoint, teaching thermodynamics and thermal systems in engineering programs often remains challenging due to the abstract nature of the concepts and the limited exposure of students to real systems. To address this issue, the objective is to provide interactive laboratory sessions in which students develop component-level models of a heat pump cycle and validate them using experimentally acquired data. Several studies have shown that active and hands-on learning strategies significantly improve student engagement, conceptual understanding, and knowledge retention in engineering education [5], [6]. In particular, project-based learning (PBL) has been demonstrated to enhance system-level understanding and student autonomy [7].

Overall, this work addresses a dual objective: from a research perspective, the development and experimental validation of component-level models for an EV reversible heat pump system; and from an educational perspective, the implementation of a project-based learning approach enabling students to connect theoretical modeling with real experimental data. This creates a mutually beneficial framework for both research and education.

## 2. Test bench description

The system studied here is a reversible AC of an EV previously presented in [8]. The system is composed of three heat exchangers, a scroll compressor, valves, and an accumulator. The refrigerant used is R1234yf. A solenoid valve system is employed to switch between operating modes, as directly reversing the refrigerant flow direction is physically impractical. This is due to several constraints: the calibrated orifice tube cannot operate under bidirectional flow, and the internal heat exchangers of the HVAC system are dimensioned differently for each operating mode, which prevents reverse operation. Figure 1 and Figure 2 represent the P&ID of the test bench in heating and cooling modes, respectively.

In cooling mode, the refrigerant enters the compressor as a low-pressure vapor and is compressed to a high-pressure, high-temperature state. It then flows through the heat exchanger HTX2 without significant heat exchange, as no air is circulated through it in this mode. The refrigerant subsequently enters the condenser (HTX1), where it releases heat to the ambient air and condenses into a liquid state. After passing through the orifice tube (V1), the refrigerant undergoes a pressure drop and becomes a low-temperature two-phase mixture. It then flows through the evaporator (HTX3), where it absorbs heat from the cabin air and evaporates before returning to the compressor. An accumulator is placed upstream of the compressor to ensure a saturated vapor state at its inlet and to prevent liquid refrigerant from entering the compressor. This is particularly important as superheating cannot be actively controlled in this system, due to the absence of an expansion valve and the use of fixed orifice tubes. As a result, the accumulator guarantees stable compressor inlet conditions over a wide range of operating conditions.

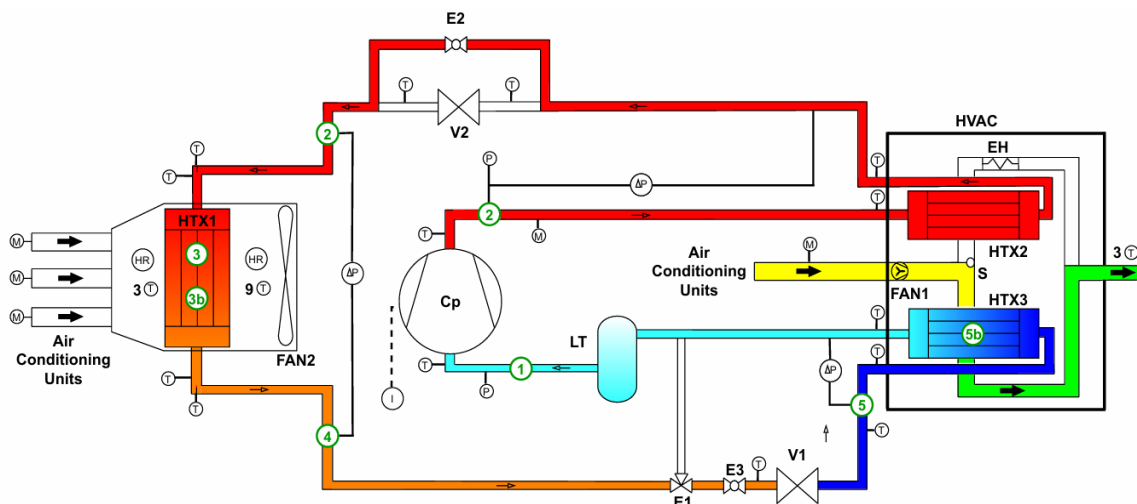
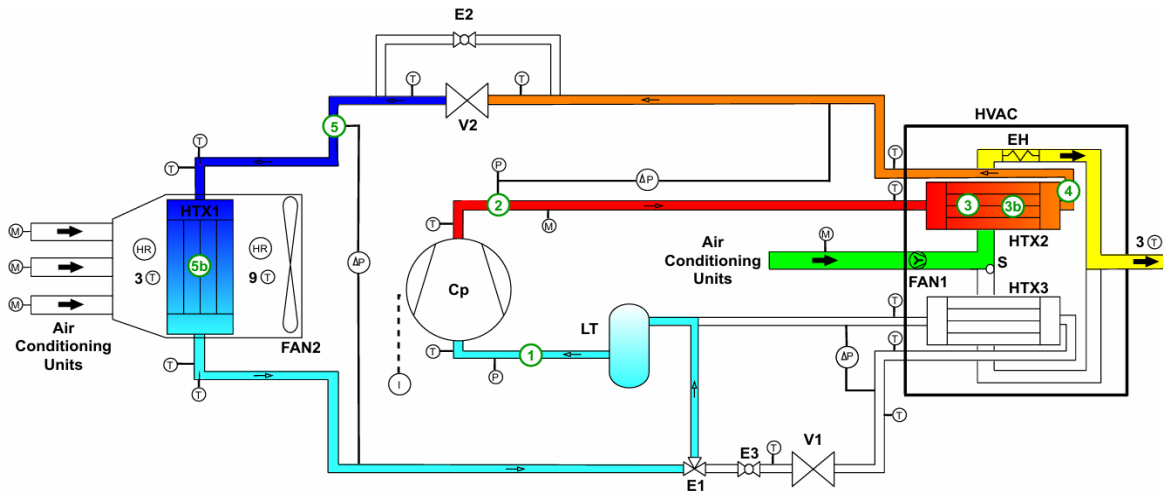


Figure 1. P&ID in cooling mode

In heating mode, the refrigerant is compressed from a low-pressure vapor to a high-pressure, high-temperature state. It then flows through the indoor heat exchanger (HTX2), where it releases heat to the air and condenses. The refrigerant subsequently passes through the orifice tube (V2), inducing a pressure drop and forming a two-phase mixture. Finally, it enters the outdoor heat exchanger (HTX1), where it absorbs heat from the ambient air and evaporates before returning to the compressor.



**Figure 2.** P&ID in heating mode

- **HTX1:** External heat exchanger
- **HTX2:** Inner condenser
- **HTX3:** Inner evaporator
- **HVAC:** Air conditioning unit of the car
- **Cp:** Compressor
- **LT:** Accumulator
- **E:** Electrovalves
- **V:** Orifice tubes
- **F:** Air fan
- **EH:** Electric heater
- **S:** Switch inside the HVAC

**Measurements:** (noted with a circle)

- Temperature (T)
- Absolute Pressure (P)
- Differential Pressure ( $\Delta P$ )
- Current (I)
- Flow meter (M)
- Relative Humidity (HR)

Air flows directions are represented by  $\rightarrow$

All components of the test bench replicate those of a commercially available B-segment electric vehicle reversible heat pump system. The only exception is the compressor, which is a PWM (Pulse Width Modulation)-controlled scroll unit with a larger displacement (34 cm<sup>3</sup> vs. 27 cm<sup>3</sup>) [9]. The test bench allows controlled operating conditions through two main variables. The compressor rotational speed is adjusted via its duty cycle. In addition, the outdoor air temperature is regulated using dedicated air conditioning units. The sensors used in this setup, including their measurement ranges and associated uncertainties, are listed in Table 1.

**Table 1.** Bench sensors characteristics

Parameter	Type	Range	Accuracy
Temperature	Type T thermocouples	[-270;370] °C	±1K
Pressure	Absolute	[0;30] bar	±0.02 bar
		[0;10] bar	±0.05 bar
	Differential	[0;1] bar	±2.5 mbar
		[0;0.5] bar	±5 mbar
Relative humidity	Humidity sensor	[0;100] %	±2% r.h
Working fluid mass flow	Coriolis	[0;1230] kg/h	±0.1% m.v.
DC current	Current sensor	[0;25] A	±0.7% f.s.

### 3. Methodology and Modelling

Within the framework of a course dedicated to thermal systems, students are tasked with developing and validating component-level models of a heat pump system. Each student focuses on a specific component, such as a compressor or a heat exchanger, and develops a physically based model using experimental data collected during laboratory sessions on the dedicated test bench. The models are implemented in Engineering Equation Solver (EES) and calibrated through comparison with measured data. In a broader perspective, these individual models are intended to be integrated into a complete system-level model.

#### 3.1 Heat exchanger modelling approach

The modelling of the heat exchangers (HTX1, HTX2, and HTX3) is based on a simplified moving-boundary (three-zone) approach adapted from the methodology described in [10]. The level of complexity is intentionally reduced to make the model suitable for student implementation during laboratory sessions. Students are required to acquire their own experimental data and use it to develop and parameterize the model of one selected heat exchanger.

Although the heat exchangers are fin-and-tube heat exchangers, they are modelled as counter-flow heat exchangers to simplify the analysis. The exchanger is divided into three distinct zones; liquid zone, two-phase zone and vapor zone. Each zone is characterized by a heat transfer area ( $A_i$ ) and an overall heat transfer coefficient  $U_i$ . For each zone, the overall heat transfer coefficient is calculated by considering two convective resistances in series (refrigerant side and air side):

$$U_i = \left( \frac{1}{h_{r,i}} + \frac{1}{h_a} \right)^{-1}$$

The refrigerant-side heat transfer coefficient varies depending on the phase:

- $h_{r,l}$ : liquid zone
- $h_{r,tp}$ : two-phase zone
- $h_{r,v}$ : vapor zone

These coefficients depend on the refrigerant mass flow rate and are estimated using:

$$h_r = h_{r,n} \cdot \left( \frac{\dot{m}_r}{\dot{m}_{r,ref}} \right)^a$$

where

- $\alpha_{r,n}$  is the nominal value
- $\dot{m}_{r,ref}$  is the reference mass flow rate (typically the average of experimental measurements)
- $a$  is an empirical coefficient (initially set to 0,8)

For each zone, the thermal conductance  $AU$  is determined using the Log Mean Temperature Difference (LMTD) method:

$$AU = \frac{\dot{Q}}{\Delta T_{log}}$$

Using the calculated  $U_i$  and  $AU_i$ , the corresponding heat transfer area for each zone is obtained:

$$A_l = \frac{AU_l}{U_l} \quad A_{tp} = \frac{AU_{tp}}{U_{tp}} \quad A_v = \frac{AU_v}{U_v}$$

The total heat transfer area of the heat exchanger is then expressed as:

$$A_{tot} = A_l + A_{tp} + A_v$$

The nominal heat transfer coefficients ( $h_{r,l,n}$ ,  $h_{r,tp,n}$ ,  $h_{r,v,n}$ ,  $h_a$ ) are not known a priori and must be calibrated using experimental data collected by the students during laboratory sessions. The calibration consists in adjusting the nominal heat transfer coefficients so that the calculated heat transfer area matches the measured one over all experimental points. During the laboratory session, the students first determine the effective heat transfer  $A_{eff,meas}$  from direct physical measurements of the heat exchanger. Then, using the previously described model and the measured operating conditions as inputs, they compute the corresponding heat transfer area  $A_{eff,calc}$ . Figure 3 presents a schematic representation of the model. The experimental measurements (shown in blue) are used as inputs for the calibration, the model parameters to be calibrated (shown in green) are the nominal heat transfer coefficients, and the model output (shown in red) is the calculated effective heat transfer area  $A_{eff,calc}$ .

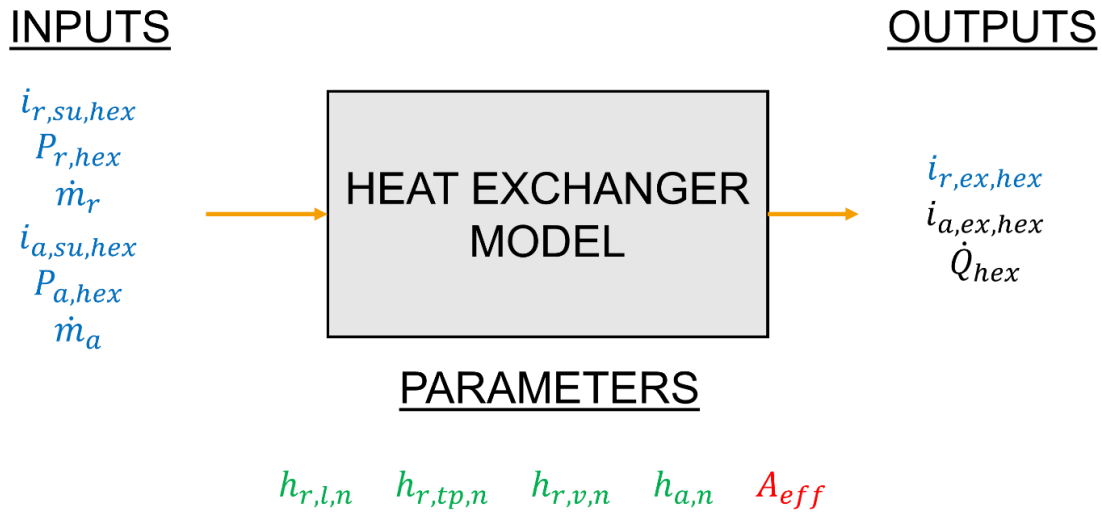


**Figure 3.** Information diagram of the heat exchanger model. The experimental measurements are shown in blue, the parameters to calibrate are shown in green and the output in red.

For a given set of parameters, the model is evaluated for each experimental point  $i$ , yielding  $A_{eff,calc,i}$ . A global error function is then defined as:

$$error = \sum_{i=1}^N A_{eff,meas} - A_{eff,calc,i}$$

where  $N$  is the number of experimental points.

After calibration of the nominal convective heat transfer coefficients, the model can be used to predict the exhaust enthalpies of both the refrigerant and the air. Figure 4 and Figure 5 compare the refrigerant exhaust enthalpies calculated by the model with the corresponding experimental values for all operating points. The results concern only the heating mode of the reversible AC system. A good agreement is observed between the simulated and measured values, with all the data points lying within the  $\pm 10\%$  deviation band, indicating that the model is able to accurately predict the outlet enthalpies.

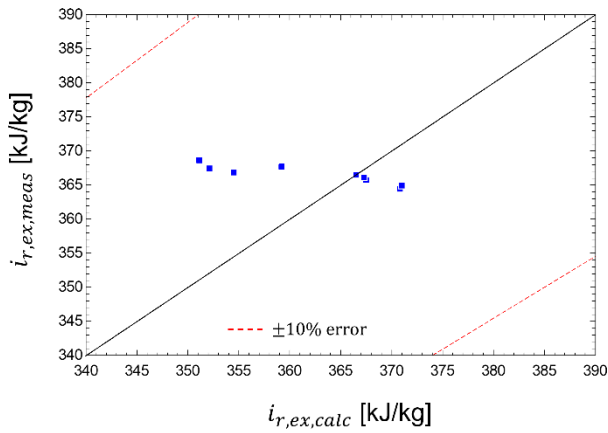


**Figure 4.** Parity plots of the measured enthalpies versus the calculated enthalpies for HTX2 (heating mode).

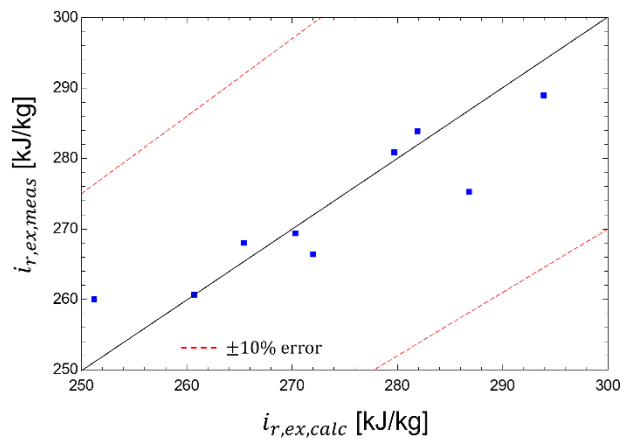


**Figure 5.** Parity plots of the measured enthalpies versus the calculated enthalpies for HTX1 (heating mode).

### 3.2 Compressor modelling approach

The compressor is modeled using a semi-empirical approach based on the methodology proposed by [11]. This type of model combines physical relationships with empirical parameters, allowing an accurate representation of the compressor behavior while remaining suitable for student implementation. The model uses measured operating conditions as inputs and predicts the refrigerant mass flow rate, discharge temperature, and compressor power consumption. A schematic representation of the model, including inputs, outputs, and parameters, is presented in Figure 6.

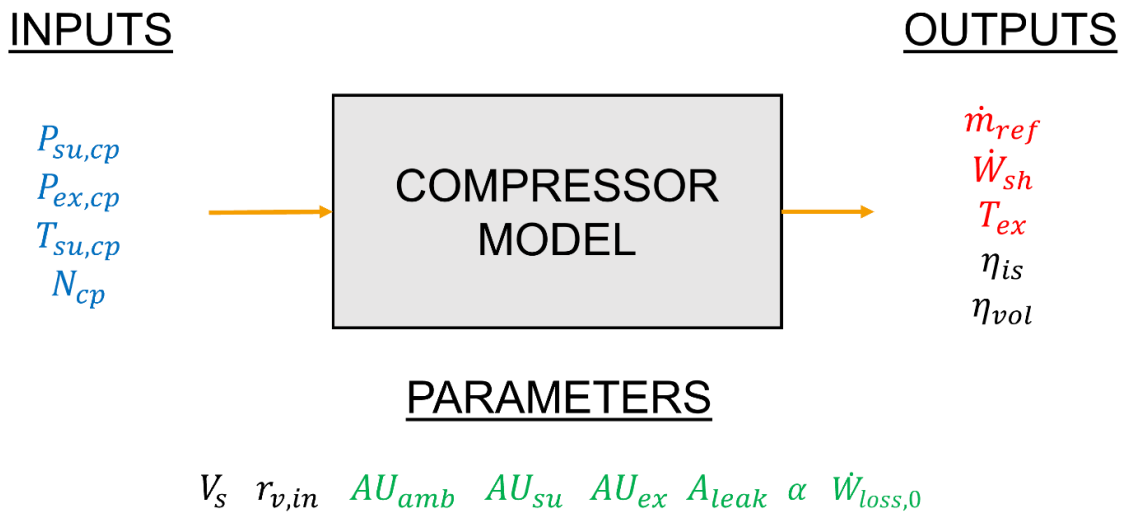


**Figure 6.** Information diagram of the compressor model. The experimental measurements are shown in blue, the parameters to calibrate are shown in green and the output in red.

The model includes several parameters that must be calibrated using experimental data, namely:  $AU_{amb}$ ,  $AU_{su}$ ,  $AU_{ex}$ ,  $A_{leak}$ ,  $\alpha$ , and  $\dot{W}_{loss,0}$ . These parameters account for heat transfer, internal leakage and mechanical losses within the compressor. The calibration is performed using an optimization-based approach. An objective function is defined to quantify the deviation between model predictions and experimental measurements. It includes the normalized errors on compressor power consumption, discharge temperature, and refrigerant mass flow rate:

$$\text{error} = \frac{1}{3N} \sum_{i=1}^N \left[ \frac{|W_{cp,calc,i} - W_{cp,meas,i}|}{W_{cp,meas,i}} + \frac{|T_{ex,calc,i} - T_{ex,meas,i}|}{T_{ex,meas,i}} + \frac{|\dot{m}_{r,calc,i} - \dot{m}_{r,meas,i}|}{\dot{m}_{r,meas,i}} \right]$$

where  $N$  is the number of experimental points.

The model parameters are identified by minimizing this error function over the full set of experimental data. Once calibrated, the model is able to reproduce the main performance characteristics of the compressor under different operating conditions.

The performance of the calibrated compressor model is evaluated by comparing the simulated outputs with the corresponding experimental measurements over the full range of operating conditions. Figure 7 to Figure 9 present parity plots for the compressor power consumption, refrigerant mass flow rate, and discharge temperature, respectively. For the compressor power consumption (Figure 7), the model predictions are in good agreement with experimental measurements, with most operating points remaining within a  $\pm 10\%$  error band. A similar trend is observed for the discharge temperature (Figure 8), where the model accurately captures the main operating behavior and remains within the same uncertainty range.

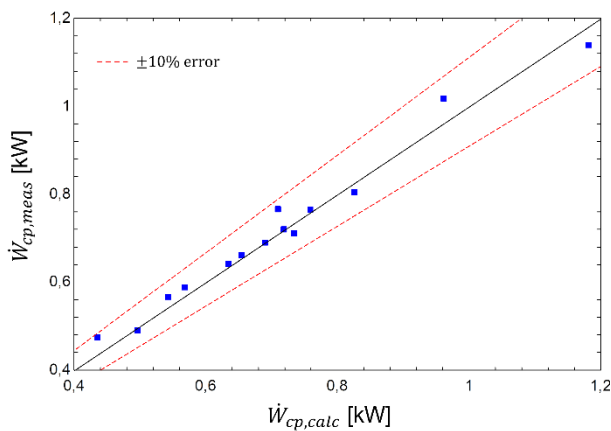


**Figure 7.** Parity plots of the measured compressor work versus the calculated one.

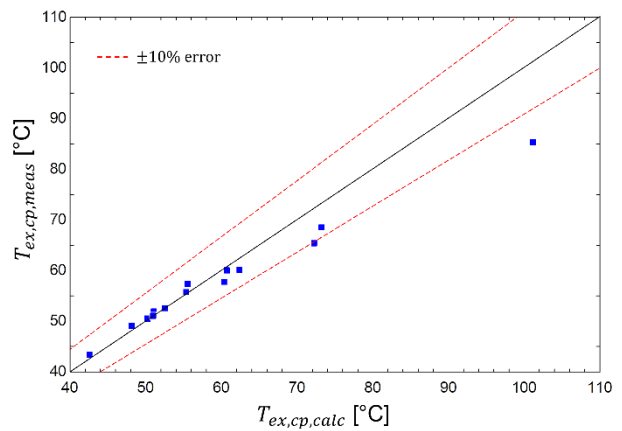


**Figure 8.** Parity plots of the measured exhaust temperature mass flow rate work versus the calculated one.

However, a larger deviation is observed for the refrigerant mass flow rate (Figure 9), where the model shows a reduced predictive accuracy and several points fall outside the  $\pm 10\%$  error band. This indicates that the mass flow rate is more sensitive to model assumptions and calibration parameters than the other variables.

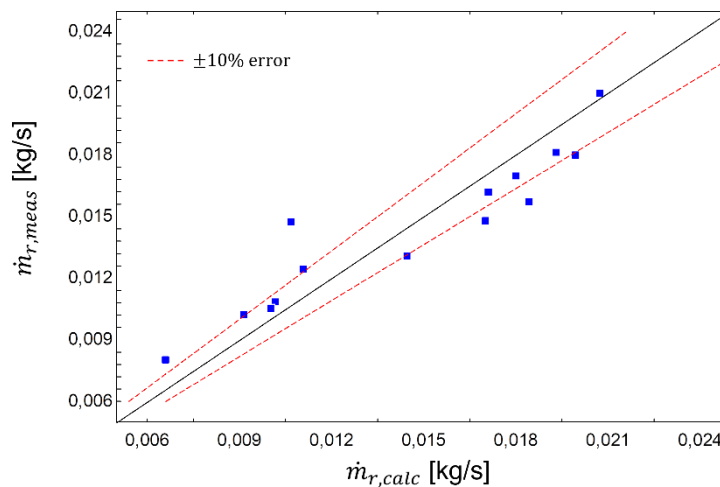


**Figure 9.** Parity plots of the measured refrigerant versus the calculated one.

### 3.3 System modelling

The component-level models developed in this work will be integrated into a complete system-level model of the reversible heat pump. This model will include additional components such as the accumulator and the orifice tubes, in order to represent the full cycle behavior. The integration of the different sub-models will be carried out in a Python environment using the open-source library LaboThApPy [12], developed at the laboratory. This framework will allow the assembly of the complete system model and the simulation of the full thermodynamic cycle of the heat pump. Figure 10 illustrates the structure of the complete system model and the coupling between the different components.

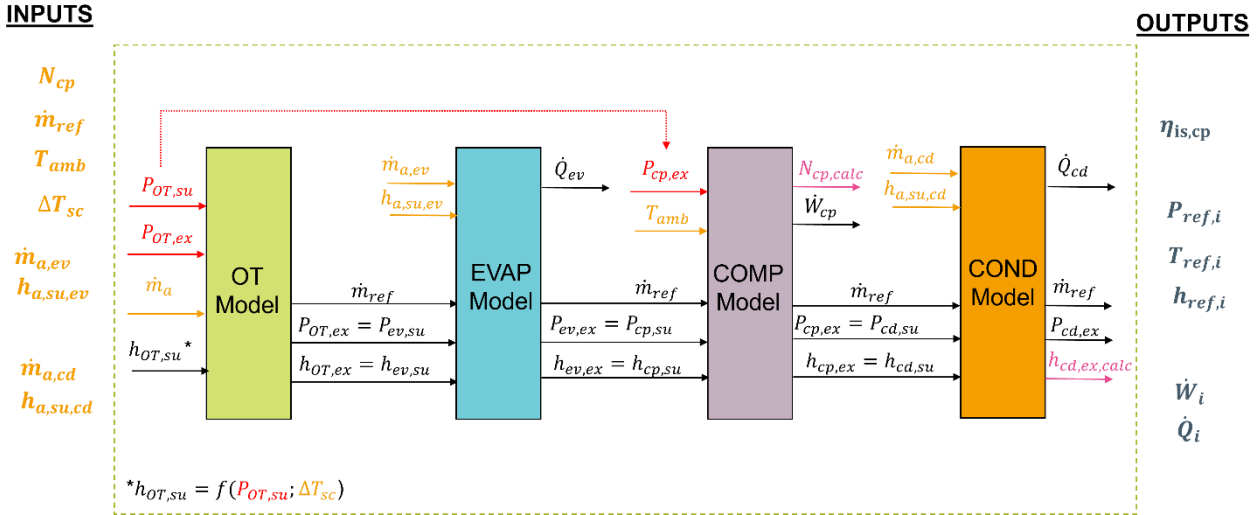


**Figure 10.** Solver architecture of the reversible AC. System inputs are in orange, guesses in red, and values used to determine residuals in pink.

## 4. Conclusion and Perspectives

This paper presented the development of component-level models of a reversible AC system for an EV, along with their calibration and experimental validation using data obtained from a dedicated test bench. The modeling approach focused on key components of the system, namely the heat exchangers and the compressor. The results show that the proposed modeling approach is able to accurately reproduce the main performance trends of the system components. In particular, good agreement between simulated and measured data was obtained for compressor power consumption and discharge temperature, while larger deviations were observed for the refrigerant mass flow rate. In addition, the heat exchanger models demonstrated good predictive capability.

From an educational perspective, this work highlights the effectiveness of a project-based learning framework in which students actively develop, calibrate, and validate models using real experimental data. This approach enables a strong connection between theoretical concepts and practical applications in thermal system engineering. Future work will focus on integrating the different component-level models into a complete system-level model of the heat pump. This will be achieved by implementing the models in a Python environment and assembling them using the open-source library LaboThApPy. Additional components, such as the accumulator and expansion devices, will be included to represent the full thermodynamic cycle. This development will enable more comprehensive simulations and support both research and educational applications.

# Nomenclature

## Symbols

$A$	area, m <sup>3</sup>
$AU$	heat transfer coefficient, W/K
$h$	heat transfer coefficient, W/(m <sup>2</sup> K)
$i$	specific enthalpy (J/kg)
$\dot{m}$	mass flow rate, kg/s
$N$	rotational speed, rpm
$T$	temperature, °C
$P$	pressure, bar
$\dot{Q}$	heat transfer rate, kW
$V_s$	swept volume, m <sup>3</sup>
$\dot{W}$	electrical power, kW

## Subscripts

a	air
amb	ambient
calc	calculated
cd	condenser
cp	compressor
ev	evaporator
ex	exhaust
$n$	nominal
r	refrigerant
su	supply
OT	orifice tube
meas	measured

## Acronyms:

AC	air conditioning
EV	electric vehicle
PBL	project based learning
PWM	pulse width modulation

# References

- [1] 'Greenhouse gas emissions from transport in Europe'. Accessed: Nov. 17, 2025. [Online]. Available: <https://www.eea.europa.eu/en/analysis/indicators/greenhouse-gas-emissions-from-transport>
- [2] S. Kalweit, E. Zeyen, and M. Victoria, 'Endogenous transformation of land transport in Europe for different climate targets', *Energy Convers. Manag.*, vol. 344, p. 120203, Nov. 2025, doi: 10.1016/j.enconman.2025.120203.
- [3] M. Kılıç and M. Ö. Korukçu, 'The Effect of Energy Management in Heating–Cooling Systems of Electric Vehicles on Charging and Range', *Appl. Sci.*, vol. 14, no. 15, p. 6406, Jan. 2024, doi: 10.3390/app14156406.
- [4] A. König, S. Mayer, L. Nicoletti, S. Tumphart, and M. Lienkamp, 'The Impact of HVAC on the Development of Autonomous and Electric Vehicle Concepts', *Energies*, vol. 15, no. 2, p. 441, Jan. 2022, doi: 10.3390/en15020441.
- [5] M. Prince, 'Does Active Learning Work? A Review of the Research', *J. Eng. Educ.*, vol. 93, no. 3, pp. 223–231, 2004, doi: 10.1002/j.2168-9830.2004.tb00809.x.

- [6] S. Freeman *et al.*, 'Active learning increases student performance in science, engineering, and mathematics', *Proc. Natl. Acad. Sci.*, vol. 111, no. 23, pp. 8410–8415, Jun. 2014, doi: 10.1073/pnas.1319030111.
- [7] J. Rodríguez, A. Laverón-Simavilla, J. M. Del Cura, J. M. Ezquerro, V. Lapuerta, and M. Cordero-Gracia, 'Project Based Learning experiences in the space engineering education at Technical University of Madrid', *Adv. Space Res.*, vol. 56, no. 7, pp. 1319–1330, Oct. 2015, doi: 10.1016/j.asr.2015.07.003.
- [8] M. Peeters, E. Neven, V. Lemort, and S. Gendebien, 'Development of a test bench for characterizing the air-to-air heat pump of an electric vehicle', 2026.
- [9] T. Gillet, 'Étude expérimentale et modélisation numérique d'un système de climatisation multi-évaporateurs pour véhicule électrifié'.
- [10] C. Cuevas, J. Lebrun, V. Lemort, and P. Ngendakumana, 'Development and validation of a condenser three zones model', *Appl. Therm. Eng.*, vol. 29, no. 17–18, pp. 3542–3551, Dec. 2009, doi: 10.1016/j.applthermaleng.2009.06.007.
- [11] V. Lemort, S. Quoilin, C. Cuevas, and J. Lebrun, 'Testing and modeling a scroll expander integrated into an Organic Rankine Cycle', *Appl. Therm. Eng.*, vol. 29, no. 14–15, pp. 3094–3102, Oct. 2009, doi: 10.1016/j.applthermaleng.2009.04.013.
- [12] E. Neven, B. Chaudoir, and V. Lemort, 'LABOTHAPPY: DEVELOPMENT OF AN OPEN-SOURCE PYTHON LIBRARY FOR THERMODYNAMIC SYSTEM MODELLING AND SIMULATION'.